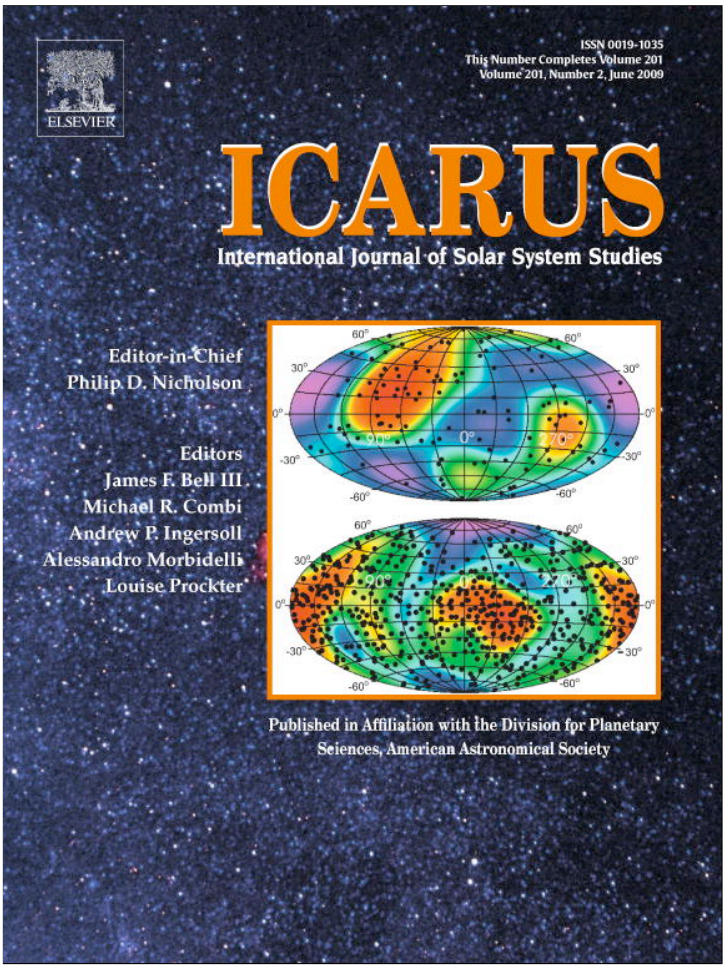

Icarus 201 (2009) 492–503

Contents lists available at ScienceDirect

Icarus

www.elsevier.com/locate/icarus

Recent rheologic processes on dark polar dunes of Mars: Driven by interfacial water?

A. Kereszturi [a,g,h,*], D. Möhlmann [b], Sz. Berczi [a,c], T. Ganti [a], A. Kuti [e,g], A. Sik [a,d], A. Horvath [a,f]

[a] Collegium Budapest, Institute for Advanced Study, H-1041 Budapest, Szentharomsag 2, Hungary
[b] DLR Institut für Planetenforschung, D-12489 Berlin, Rutherfordstr. 2, Germany
[c] Eotvos Lorand University of Sciences, Institute of Physics, H-1117 Budapest, Pazmany 1/A, Hungary
[d] Eotvos Lorand University of Sciences, Institute of Geography and Earth Sciences, H-1117 Budapest, Pazmany 1/c, Hungary
[e] Eotvos Lorand University of Sciences, Institute of Physics, Department of Astronomy, H-1117 Budapest, Pazmany 1/c, Hungary
[f] Konkoly Observatory, H-1525 Budapest, Pf. 67, Hungary
[g] Hungarian Astronomical Association, H-1461 Budapest, Pf. 219, Hungary
[h] Karoly Nagy Astronomical Foundation, H-1011 Budapest, Szekely u. 2–4, Hungary

ARTICLE INFO

Article history:
Received 16 September 2008
Revised 27 January 2009
Accepted 27 January 2009
Available online 31 January 2009

Keywords:
Mars, surface
Ices

ABSTRACT

In springtime on HiRISE images of the Southern polar terrain of Mars flow-like or rheologic features were observed. Their dark color is interpreted as partly defrosted surface where the temperature is too high for CO_2 but low enough for H_2O ice to be present there. These branching streaks grow in size and can move by an average velocity of up to about 1 m/day and could terminate in pond-like accumulation features. The phenomenon may be the result of interfacial water driven rheologic processes. Liquid interfacial water can in the presence of water ice exist well below the melting point of bulk water, by melting in course of interfacial attractive pressure by intermolecular forces (van der Waals forces e.g.), curvature of water film surfaces, and e.g. by macroscopic weight, acting upon ice. This melting phenomenon can be described in terms of "premelting of ice". It is a challenging consequence, that liquid interfacial water unavoidably must in form of nanometric layers be present in water ice containing soil in the subsurface of Mars. It is the aim of this paper to study possible rheologic consequences in relation to observations, which seem to happen at sites of dark polar dunes on Mars at present. The model in this work assumes that interfacial water accumulates at the bottom of a translucent water-ice layer above a dark and insolated ground. This is warmed up towards the melting point of water. The evolving layer of liquid interfacial water between the covering ice sheet and the heated ground is assumed to drive downward directed flow-like features on slopes, and it can, at least partially, infiltrate (seep) into a porous ground. There, in at least temporarily cooler subsurface layers, the infiltrated liquid water refreezes and forms ice. The related stress built-up is shown to be sufficient to cause destructive erosive processes. The above-mentioned processes may cause change in the structure and thickness of the covering ice and/or may cause the movement of dune grains. All these processes may explain the observed springtime growing and downward extension of the slope streaks analyzed here.

1. Introduction

Bulk water cannot stably exist at the thermodynamic conditions in a broad range of subzero-temperatures present on Mars. However, liquid interfacial water must stably exist at these temperatures also in the subsurface of Mars if the soil contains ice (Möhlmann, 2004) and ice must be present in the uppermost surface due to adsorption and freezing of atmospheric water vapor, and/or the ice may also be a subsurface relict of earlier water rich martian epochs. Salts may influence the upper situation, and some models suggest water may be ephemerally present (Clow, 1987; Haberle et al., 2001; Hecht, 2002) or even flow (Motazedian, 2003) on Mars today.

Liquid interfacial water in the H_2O-ice containing parts of the subsurface of Mars today may be related to physical, chemical, and eventually also to biological processes (Möhlmann, 2008). The presence of this interfacial water may be enhanced and extended to lower temperatures in brines of various salts (Mellon and Phillips, 2001; Knauth and Burt, 2002) and may help destabilizing slope materials (Kossacki and Markiewicz, 2008). Brass (1980) analyzed the freezing point of various salt–water systems on Mars and suggested freezing point may be as low as 225 K. Interesting analogues have been discovered in the Antarctica Dry Valleys with some liquid water related structures, resem-

* Corresponding author at: Collegium Budapest, Institute for Advanced Study, H-1041 Budapest, Szentharomsag 2, Hungary.
E-mail address: akos@colbud.hu (A. Kereszturi).

0019-1035/$ – see front matter
doi:10.1016/j.icarus.2009.01.014

bling to martian low latitude slope streaks (Head et al., 2007a, 2007b).

2. Types of ices and frost in the analyzed terrains

It is important to distinguish between the two kinds of ice covering the martian surface: carbon dioxide ice and water ice. The structure of these ice types (slab or porous) is not well known, however it is possible to distinguish between the water and carbon dioxide ices on the basis of their spectra, albedo and related surface temperature together. In this work, we analyzed terrains by using satellite-born images, and TES albedo and temperature values. In every case we have indicated, which type of ice is probably on the surface, and which parameters suggest the presence of that one, and the absence of the other kind of ice.

Hereafter first we present the observations and description of polar springtime surface features, where springtime insolation gives rise to strange features resembling to those caused by a flowing liquid. In the second part, a theoretical and modeling background to describe these recent rheological phenomena is given, which is based on the at least temporary presence of interfacial water in the uppermost surface layers. Detailed information about the formation of this interfacial and adsorbed water layer on the soil grains can be found in the references, here we only present some basic formulas in connection with the observed structures.

The frost cover and its sublimation play an important role in the interpretation of our observations. Both water and carbon dioxide ice can be present on the martian surface inside the seasonal caps. At the Northern Polar Region water ice forms a wide annulus at the perimeter of the receding seasonal carbon dioxide ice cover (Kieffer and Titus, 2001; Bibring et al., 2005; Schmitt et al., 2005; Schmitt et al., 2006), partly because it appears from below the sublimated carbon dioxide seasonal cap and partly because it recondenses onto the perimeter of the remaining carbon dioxide ice (Wagstaff et al., 2008). Opposite to this situation at north, no similar water ice annulus was observed at the Southern Polar Region, only smaller water ice patches (Titus, 2005; Langevin et al., 2006; Titus, 2008) are present, which appear at the perimeter of the receding annular carbon dioxide cap, and somewhere they are tens of kilometers away from the bright permanent cap (Bibring et al., 2004) in summertime.

These observations can be interpreted, by assuming that a thin water ice layer below the seasonal carbon dioxide frost is present, and water ice is left behind the sublimating carbon dioxide ice cover. Such stratigraphy can be expected from theoretical reasons, too: when seasonal cooling starts, ice condenses on the surface first from the cooling atmospheric water vapor, and carbon dioxide (by its lower frost temperature) condenses later, forming a layered structure. At the landing site of the Phoenix probe also water ice frost appeared first with the cooling temperature in autumn (Lunar and Planetary Laboratory Press Release) as it was too warm there to see any dry ice. This frost probably formed by direct condensation from the atmosphere, although falling snowflakes were also observed by LIDAR on Phoenix (NASA Press Release, 2008).

The mentioned above observations and theoretical assumptions suggest that at polar terrains on Mars, when the temperature is above the carbon dioxide frost point, and as long as the surface is still frost covered, this frost is water ice.

3. Appearance of the possible seepage features

We observed dark slope structures emanating from Dark Dune Spots (DDSs) in the southern terrain on MGS MOC (Horvath et al., 2001), and MRO HiRISE images. DDSs are a special class of polar seasonal albedo features, their basic characteristics are the following: they are round shaped low albedo structures on the seasonal frost-covered surface of dark dunes, appear late winter, grow in size and number, and finally disappear with the disappearance of seasonal frost in early summer. They are present in the Southern hemisphere between 65 and 80 degrees of latitude. (Although resembling seasonal dark albedo structures are present in the northern hemisphere too, they are excluded this work.)

The most important features related to DDSs are the elongated slope streaks (Horvath et al., 2001; Ganti et al., 2003; Szathmary et al., 2005). These slope structures always start from these spots, at the analyzed terrain. These spots form special groups among the various ephemeral seasonal albedo structures on Mars observed by different authors (Christensen et al., 2005; Kieffer, 2003; Malin and Edgett, 2000; Piqueux et al., 2003).

DDSs generally show internal structures with a darker (umbra-like) central part, surrounded by a lighter, outer (penumbra-like) ring — although there are many irregular shaped spots among them. Their diameters vary between 5 and 200 m; and have a yearly reoccurrence to a degree of 50–65%, meaning that about half of the spots appear very close (in meter scale distance) to the location of spots from the previous year. Their most interesting aspect analyzed in this work is the elongated structures on slopes, emanating from them.

Dark Dune Spots were analyzed previously on MGS MOC images (Horvath et al., 2001; Ganti et al., 2003, 2006; Kereszturi et al., 2007; Szathmary et al., 2007). Based on the comparison of morphology, location and seasonal appearance of seasonal dark spots on new HiRISE and earlier MOC images, we suggest the dark spots and slope structures observed in the HiRISE images represent the same phenomena as earlier noted on MOC images (Fig. 1).

The streaks emanating from these spots, form two groups. The larger group consists of diffuse, fan shaped streaks, probably formed by the combination of CO_2 geyser activity and winds (Kieffer et al., 2006) on slopes and horizontal terrains too. The second group has a confined appearance (we call them confined streaks hereafter), which evolves during a later seasonal phase. These are seen only on slopes (Kereszturi et al., 2007, 2008), when the surface temperature is sufficiently high, and consequently less or no CO_2 ice cover is present.

The temperature values during this later seasonal phase are too high for the carbon dioxide ice to cover the whole observed area. Unfortunately the spatial resolution of TES temperature data is not high enough to observe precisely the area of these dark structures, so we cannot determine are they free of CO_2 ice, but it is highly probable. If the temperature of a kilometer sized terrain is higher than the CO_2 frost point, then CO_2 frost free areas can be expected to exist. The mentioned above dark features must absorb more sunlight than their surroundings, so they must be warmer than the average temperature of the observed area. Because of this and the earlier observations of stratigraphic relationship of H_2O ice below CO_2 ice (see Section 2), it is possible that CO_2 ice is absent in the spots, and water ice left behind because of the above mentioned layered structure.

On the analyzed HiRISE images both of the upper mentioned two slope streak groups, the diffuse and the confined were also identified, as well on MOC images. On HiRISE images the diffuse streaks turned out to consist of small (0.2–2 m) dark patches that form a discontinuous fan-shaped structure. These small patches were visible as coalesced, continuous diffuse fans in the lower resolution images of MGS MOC. The confined streaks, seen already on MGS MOC images, look like continuous dark streaks on HiRISE images too.

4. Method of slope streak analysis

For the analysis we used HiRISE (MRO), HRSC (MEX), MOC (MGS) images, with topographic data from MGS MOLA PEDR (Precision Experiment Data Record) dataset with processing version L

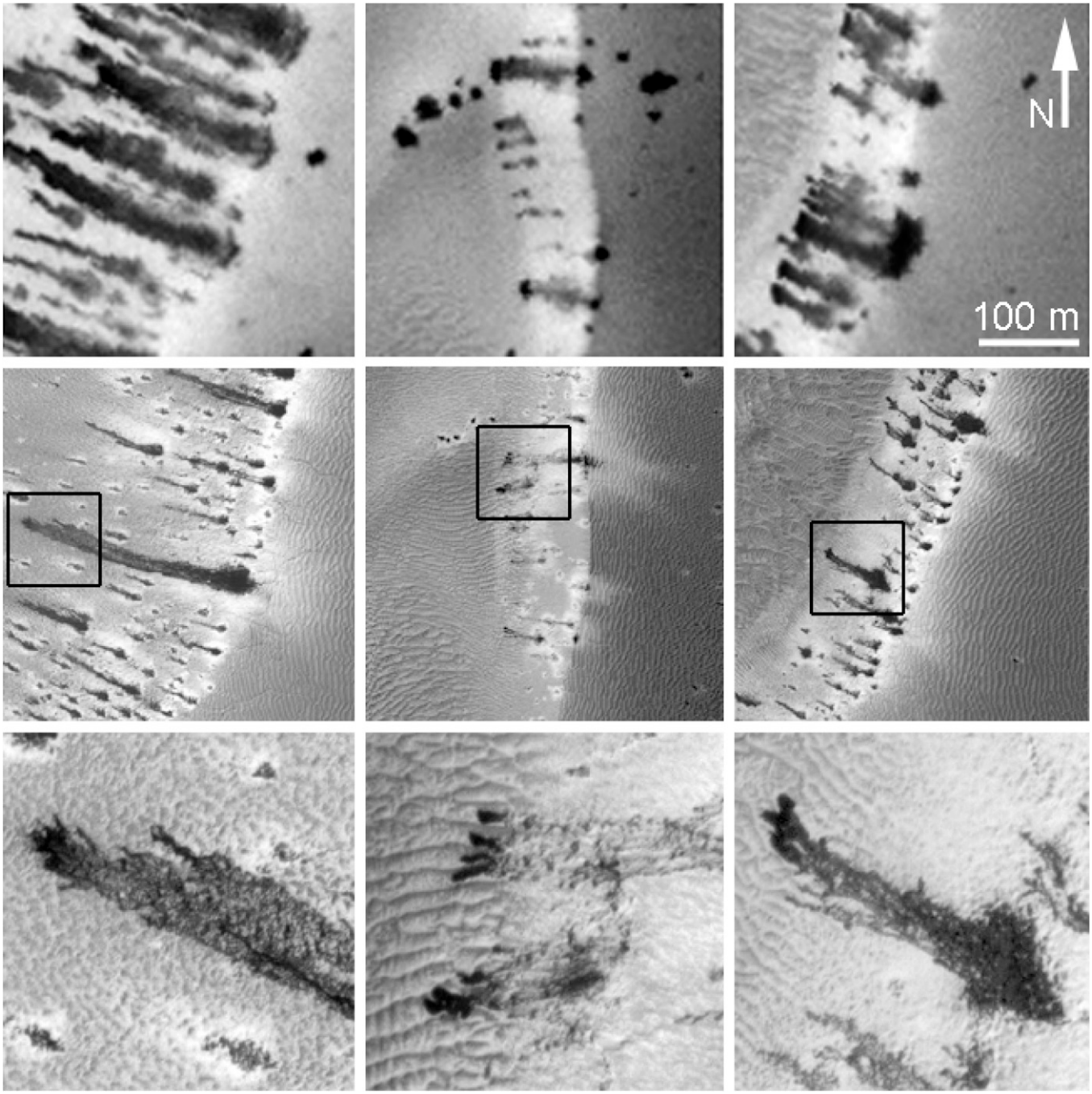

Fig. 1. Comparison of MOC (top) and HiRISE (middle, bottom) images of the same terrains at different dates, showing the similar phenomenon was observed by MGS and MRO. Top row shows 300 × 300 m insets of MGS MOC image R07-00938 (Ls = 220°), middle row shows 300 × 300 m insets of HiRISE images PSP-003609-1110 (Ls = 232°) of the same terrains. In the bottom row 80 × 80 m segments are visible in magnified version of the middle row, which locations are indicated by black boxes. North is up, the Sun illuminates from the left and slopes are tilted toward the left.

(Smith et al., 1999), and temperature data from TES (MGS) measurements (Christensen et al., 1992), using the "vanilla" software. Temperature data show annual trend, and were derived for daytime around 2 pm, local true solar time. The surface temperature values have spatial resolution of around 3 km, so they can be taken only as a rough approach of the surface temperature of the whole analyzed dune complex. Another source of uncertainty is that the temperature values were used only to realize a general annual trend. These values can be taken as an orienting approach only to the conditions at the observed locations and dates.

The change of seasonal albedo structures was analyzed on dunes inside three craters during southern spring: Russell (54S 12E), an unnamed crater (68S 2E), and Richardson (72S 180E). Only 11 of the analyzed HiRISE images of these craters showed confined slope streaks. Their parameters can be seen in Table 1.

For temperature analysis we used MGS TES bolometer data, acquired in nadir-pointing mode with "vanilla" software. Other data on martian surface temperatures could be acquired form THEMIS too, that has better spatial resolution but unfortunately observed rarely the same terrain.

During the analysis we used the following terms to characterize the structures. The term "slope streak" is used here only for those structures, which are analyzed in this paper, although in the literature it is generally used for low latitude streaks formed possibly by the mass wasting process of dust (Aharonson et al., 2003; Schorghofer et al., 2007; Beyer et al., 2008; Chuang et al., 2007).

Table 1

Crater	Image No.	Date	Ls
Russell (54S 12E)			
	2482_1255	2007.02.05 15:52	178.9
	2548_1255	2007.02.10 16:00	181.8
	2904_1255	2007.03.10 15:57	197.9
Unnamed crater (68S 2E)			
	3432_1115	2007.04.20 15:55	222.9
	3643_1115	2007.05.07 15:51	233.2
	3709_1115	2007.05.12 15:56	236.4
Richardson (72S 180E)			
	3175_1080	2007.03.31 16:08	210.6
	3386_1080	2007.04.17 16:04	220.7
	3597_1080	2007.05.03 16:00	230.9
	3742_1080	2007.05.15 15:49	238.1
	3953_1080	2007.05.31 15:42	248.5

Here it is used for elongated structures that stretch in downward direction on slopes, and emanate from DDSs. The term "movement" was used here for the description of the change in the location of dark colored surface parts, and that probably, but not necessarily means the real movement of any material. Theoretically changes in phase or color at neighboring locations can also manifest in a similar phenomenon. We used the term "flow front" for the advancing frontal section of these elongated dark slope structures, toward the direction of their movement. Rheologic term is also used for the movement of material on the surface or right below it.

5. Morphology of slope structures

The structures analyzed in this article were observed on dark dunes inside craters at the southern hemisphere. These dunes are actually complexes of smaller dune units with size of around 1 km, and the diameter of one complex is between 10 and 20 km. The smallest visible topographic structures are ripples on the top of the upper mentioned structures, with width of 5–20 m. During the observations the surface was covered with bright frost (at the beginning CO_2, later possibly somewhere only H_2O), peppered with small Dark Dune Spots and the slope features emanated from them. Analyzing nearly one hundred slope streaks on HiRISE images, a characteristic sequence of events is visible that follows each other as the season passes by. The phases of the DDS and related slope streak changes are:

1. A dark spot appears, at some occasions with fan shaped streaks emanating from it (it cannot be decided whether the spot appears first before the fan, or they appear at the same time).
2. Confined streaks start emanate from DDSs in downward direction at slopes.
3. The branching pattern of the streaks becomes more developed and the streaks become longer as time passes by. During this phase a brighter halo comes visible around both the DDS and the slope streak, possibly related to some refreezing phenomenon.
4. With the advancement of seasons (towards summer) the dark parts become gray and gradually reach the dark color of the whole dune complex.
5. The color/brightness of the whole terrain gets more and more homogeneous, and finally only small signs of the previously observed dark albedo markings remain visible.

In the second and third phases of the mentioned above sequence, slope streaks are obviously present as dark features elongated downward on the slopes. For the determination of the downward direction, we can use MOLA topography only in the cases of the largest slopes. In most of the cases, the slope direction was identified on the basis of the lighting condition, where the sunward slopes were generally brighter than the opposite ones (see Fig. 2. for examples, where the Sun illuminates from the right,

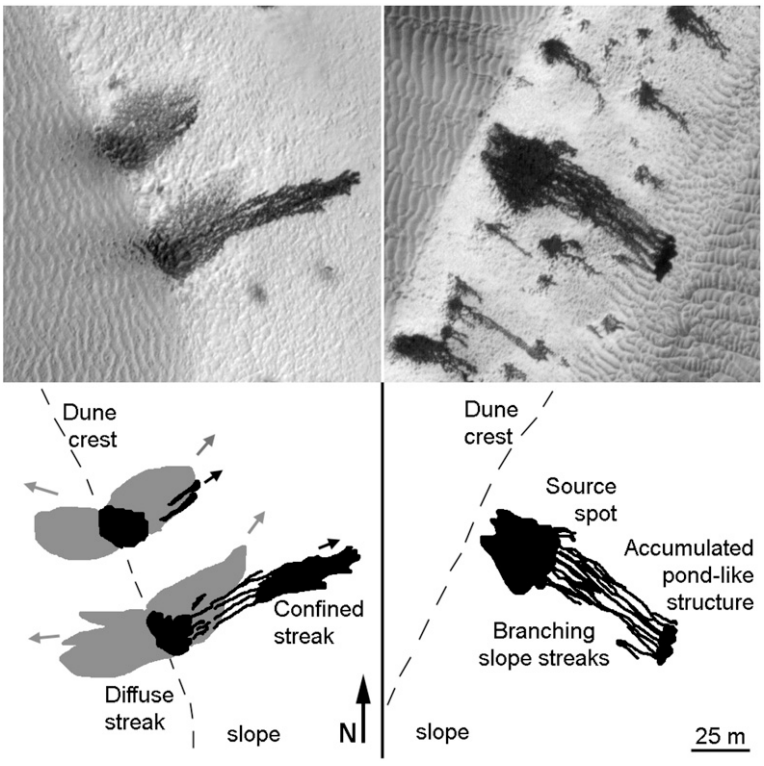

Fig. 2. Example for characteristic morphology of slope streaks. Left: distinction between fan-shaped (gray) and confined (black) slope streaks based on their appearance and direction of elongation on an 125 × 125 m part of HiRISE image No. PSP_003175_1080. Right: examples for branching morphology of streaks and accumulated pond-like termination. The images are visible up and the graphical representations at bottom.

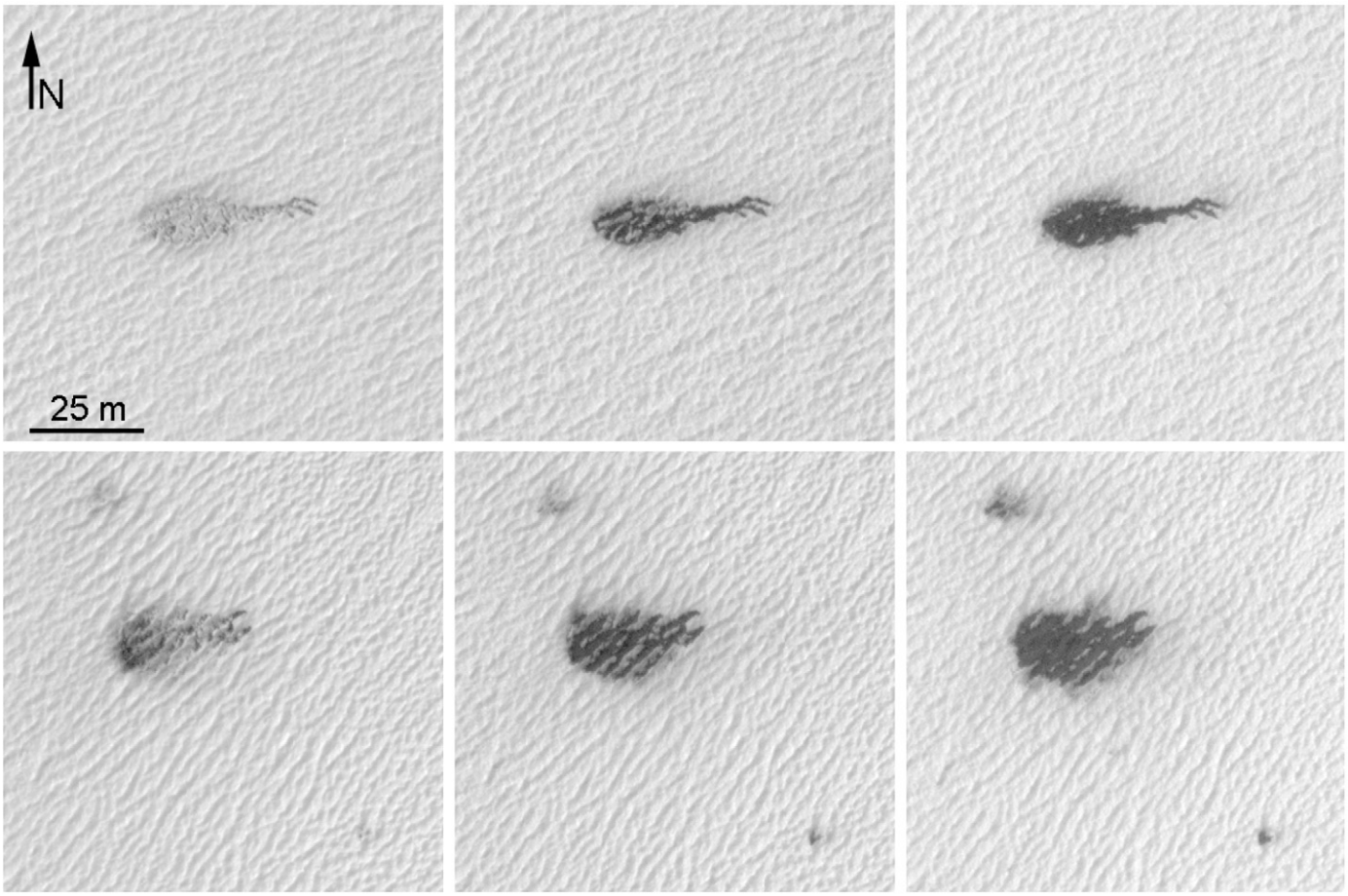

Fig. 3. Development of two passive streaks (top and bottom rows) on 100 × 100 m sections of HiRISE images No. 3432–1115, 3643–1115, 3709–1115 (from left toward right), acquired at Ls = 222.9, 233.2, 236.4 respectively. Based on the morphology they moved toward the right (toward the elongated part) previously, but currently they show only darkening and the growth of small segments, which finally coalesce into a continuous streak.

so the brighter slopes are tilted toward the right). Slope streaks were observed only at those locations where the sloping angle was high enough to produce obvious brightness differences between opposite slopes. Based on the analysis of some individual MOLA measurements, the slope angle was somewhere between 5 and 20 degrees (here the horizontal plane has 0, the vertical 90 degree of slope angle).

The confined slope streaks always follow the sloping direction, regardless to the exposure of the slope faces (e.g. north, south, east, west). No such preferred direction is visible among the differently oriented slopes, although it is worth noting that homogeneous samples may hardly exist because the dune crests in many cases are north–south oriented, probably by the general east–west winds. This suggests that the slope angle value plays stronger role, than orientation of the slope.

All the confined slope streaks visible in the mentioned above images emanate from the Dark Dune Spots in downslope direction. They have characteristic appearance: forming a branching network, where the smallest branch had a width of 3–6 m. This latter may be a characteristic value, and it is equal to the average distance between the small dune ripples, which influence their path like “channeling”. At many locations individual branches split into two branches because of obstacle-forming ripples, and there are also cases where two or more branches coalesce.

6. Movement of slope streaks

We use the term of movement for the downward stretch of the dark slope streaks emanate from Dark Dune Spots as time passes by. Regarding the movement of the low albedo slope streaks, we have observed the following:

- The dark slope streaks always start from the DDSs downward, regardless the fact, is the DDS situated at the dune crest or on the slope itself — although more DDSs are present at the top of a slope than on the slope. No streaks are visible without DDSs (except for those cases where the DDS, that probably triggered the streak formation, diminishes during the streak movement, possibly by some refreezing phenomenon). This means that the processes, which trigger the formation of slope streaks are in connection with DDSs. The reason for these processes may be related to the dark color of the DDS that supports an increase of the temperature.
- All the confined streaks stretch downward on slopes (Horvath et al., 2009), suggesting that gravity driven effects dominate the development, opposite to the gas jet process, which forms fan shaped streaks in various directions.
- The dark colored slope streaks become longer as time passes by in many cases — while there were slope streaks, which did not grow during the same period, and did not show any movement. In an earlier work (Horvath et al., 2005) we have shown that there is a statistical connection between the length of a slope structure and the size of the original DDS that may be valid here as well — although the situation seems to be more complicated for slope streaks.
- The advancing flow front follows the several meter sized furrow-like depressions between the small, probably wind-blown ripples.

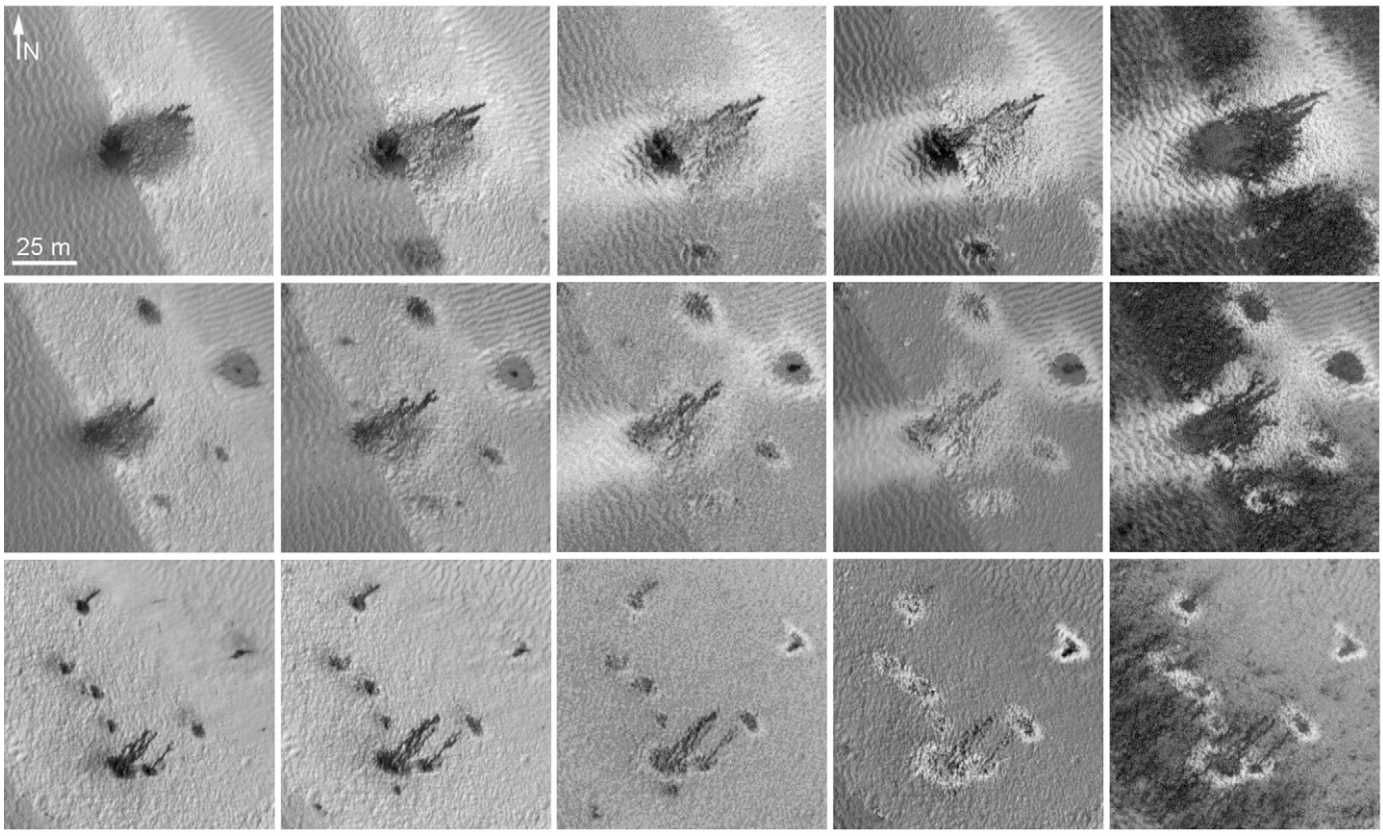

Fig. 4. Change DDSs at three locations in Richardson crater. The 100 × 100 inset pictures are from HiRISE images (from left to right image No. 3175, 3386, 3597, 3742, 3953, which were acquired at Ls = 210.6, 220.7, 230.9, 238.1, 248.5), showing the development of structures.

- During the late phase of the dark material's movement, sometimes the source region became lighter, indicating possibly that the dark material has moved away, leaving behind other stuff, or that the source region became covered by whitish frost again; or if only phase changes have caused the dark color, the phase changed back again to the original state of the source.
- The elongation of streaks takes place in the form of narrow, 2–10 m wide branches. They are usually the darkest at their flow front, and get brighter upward with time. During their advancement, in several cases the source region (the DDS itself) and the upward part of the streak become brighter as time passes by. This observation may be related to some kind of refreezing phenomena with a bright frost cover, or by the cessation of any possible phase change that produced the originally dark color.
- On the bottom of the slopes, dark pond-like structures form where the streaks arrive at a nearly horizontal surface, stop their movement, and probably accumulate and/or seep into the near surface ground.

Based on the analysis of morphology and its changes in time, we have identified two subgroups of confined streaks, emanating from dune spots: active and passive streaks (Fig. 3). We use the term "active confined streak" for such streaks, which show evident signs of gradual movement of dark fronts as the season passes by (Fig. 4). In the case of "inactive confined streaks", no similar moving flow front was observable, and only the small and separated dark parts became visible as the season passed by. With the progress of the spring season, the dark areas grow, connect the separated parts and form a continuous streak. By the end of this coalescence, the passive streak gains similar appearance to an active confined streak. The elongated morphology suggests that these streaks have already moved in the past, possibly during different climatic periods, but currently they only show a locally fixed darkening without movement.

We have measured the movement speed of the flow fronts of active streaks for several individual branches on subsequent images, where the same branch of certain slope streaks could be firmly identified. The measured values were calculated for martian days (sols) as an average value, as if the whole movement had happened during a full martian sol. If the theory described in this paper can be applied, a thin liquid film of interfacial water lubricates the grains. The resulting movement may take place only during a small part of a martian day, probably when the temperature and water content produce a sufficiently thick layer of undercooled liquid interfacial water. Also freezing may cause expansion and failure inside the dunes' structure (see Section 8.3).

The observed average motion speed of flow fronts has been estimated to be of up to 1.4 m/sol. There were many occasions where the dark stuff did not move, or moved slower than 0.1 m/sol. Where the movement was obvious, it usually happened on meter scale distance on the average on a martian day (Fig. 5). This suggests the presence of some critical limit above which the movement took place, and that it happens at a reasonable distance.

7. Connection between temperature and morphology

We have analyzed average annual TES based surface temperatures and the related morphology of the slope streaks. The three observed craters were situated at different latitude, at 54, 68 and 72° S. As a result, during the springtime warming the average surface temperature reaches certain values later in solar longitude for locations farther from the equator. If the beginning of the dark streaks' movement takes place after the temperature has reached

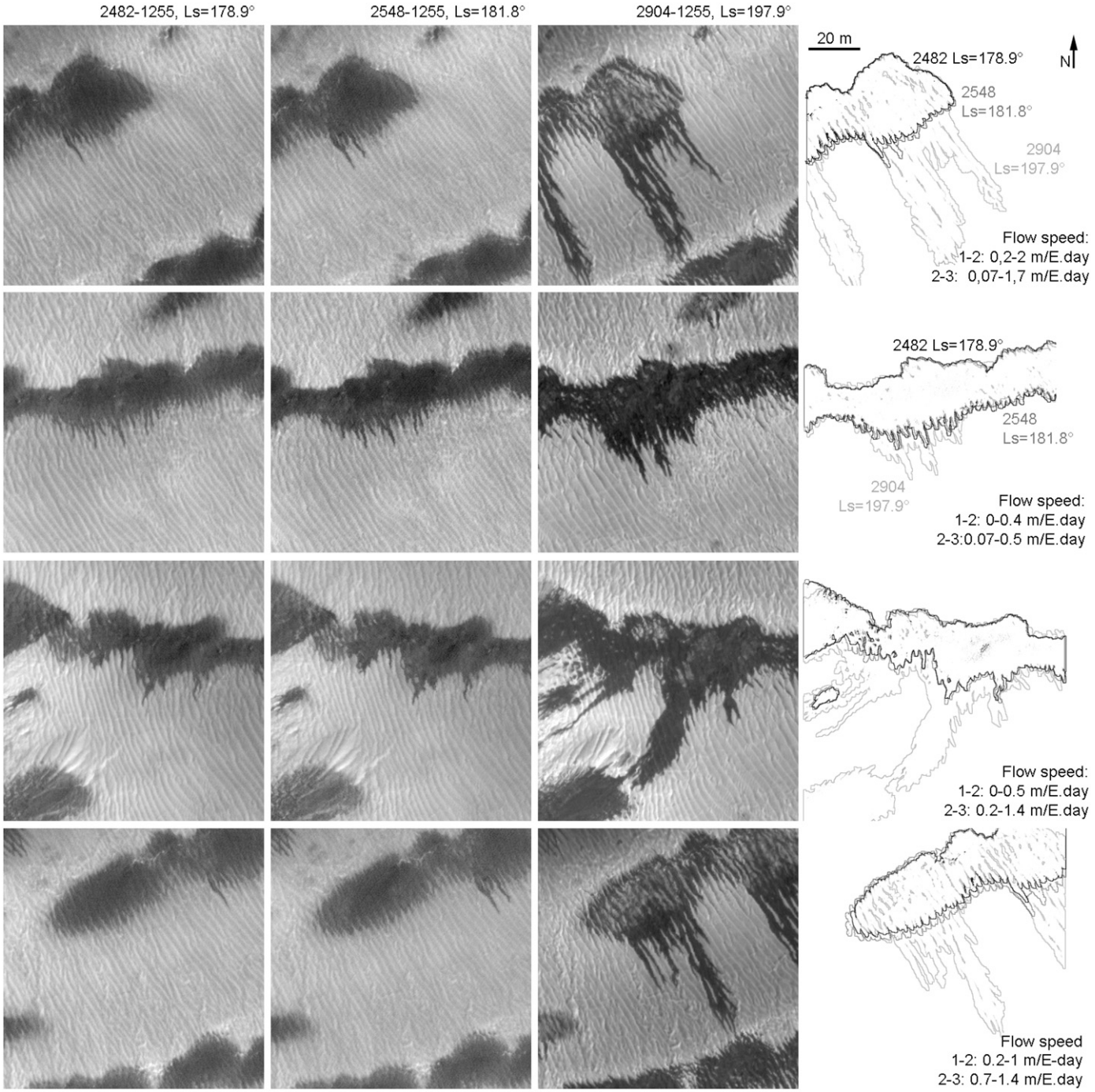

Fig. 5. Example images of active streaks from Russell crater. The three images from left to right represent subsequent HiRISE images No. 2482, 2548, 2904 which were acquired at Ls = 178.9, 181.9 and 197.9 respectively. On the right a graphical representation is visible, showing the movement and its observed speed.

a critical value, it is expected that the movement starts later closer to the south pole.

We have studied the annual temperatures (Figs. 6–8), with continuous TES based datasets, but regarding the images unfortunately there is no continuous coverage of the whole spring period available. The first indications of streak movement can be observed earlier in Richardson crater than in Russell crater, because for Russell no image is available for the critical period. So, it was not yet possible to establish a direct relation between the first appearance of streaks and the seasonal increase in temperatures.

The TES temperature values can be taken only as a rough approach for the surface temperatures. Because of the comparatively low spatial resolution of the detector, it cannot resolve certain parts of the dark features, which may be warmer than the measured "average" value. In spite of this restriction, the streaks' movement started around the same temperature in Russell, the unnamed crater, and probably in Richardson crater too, but there the situation is somewhat different, as described below in more detail.

Analyzing the average annual temperature trend and the changes in streaks' morphology, the streaks appeared in Russell and the unnamed crater when the temperature was between 180 and 200 K. In Richardson crater the situation is different: the first indication of the slope streak movement there appeared on the images acquired at Ls = 210.6, when the average temperature is not much above the frost point of carbon dioxide. But the temper-

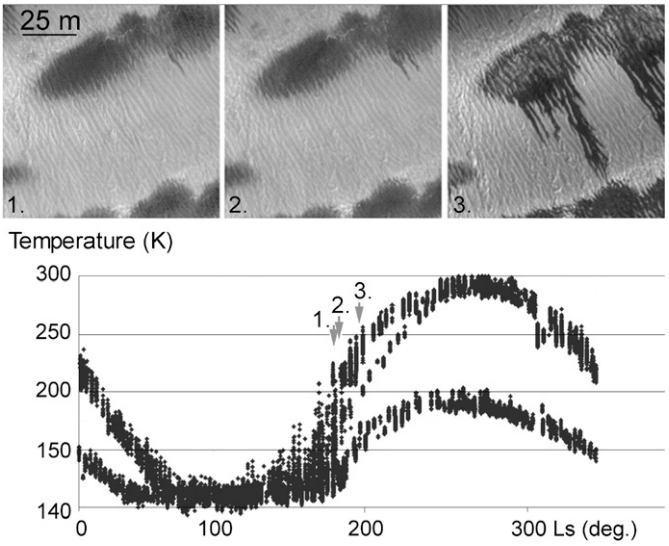

Fig. 6. Temperature-morphology correlation for Dark Dune Spots and slope streaks in Russell crater, with 100 × 100 m sized images of the same terrain are visible at top, where the number of HiRISE images from left to right are 2482–1255, 2548–1255, 2904–1255, which were acquired at Ls = 178.9, 181.8, 197.9 respectively. At bottom the temperature curve is indicated (top curve: daytime, bottom curve: nighttime values). Three vertical lines show the temperatures corresponding to the three periods of seasons at the upper images.

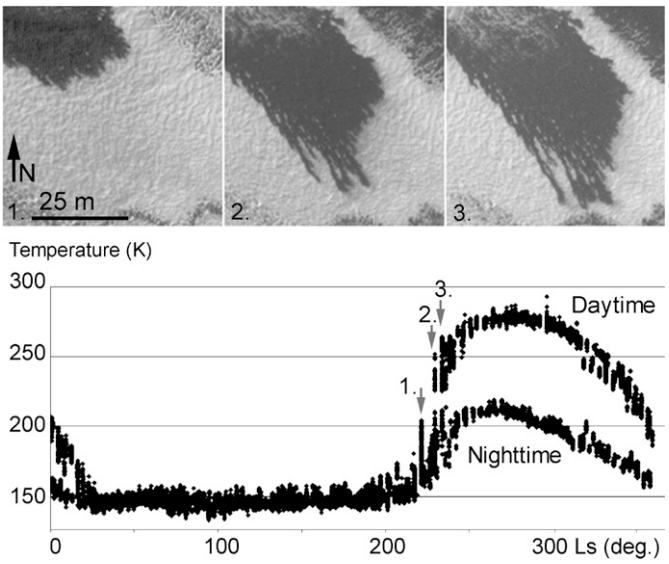

Fig. 7. Temperature-morphology correlation for Dark Dune Spots and slope streaks in an unnamed crater at 68S 2E. Three 50 × 50 m insets from HiRISE images are visible up (from left to right image No. 3432, 3643, 3709, which were acquired at Ls = 222.9, 233.2, 236.4 respectively) and TES based annual temperature values are visible below.

ature curve has already started to rise, suggesting that there must be warmer locations free of CO_2 frost on the surface, but they are probably below the limit of the spatial resolution. These warmer small patches may be the dark features, because their much lower albedo causes a warm-up in course of the increasing insolation.

In general, and based on TES temperature data, it can be stated that during the movement of slope structures, a large part of the surface (or the whole observed area) is free of carbon dioxide ice, as the temperature of the dark slopes is above the CO_2 freezing point. At the same time, based on the images, frost covers most of the terrains, so that frost is probably composed of water ice. As a conclusion the dark slope streaks are active during a seasonal phase when water ice is probably present and exposed to the surface in the analyzed regions.

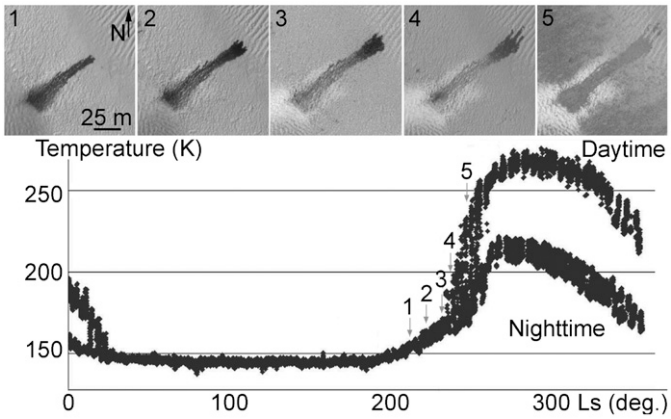

Fig. 8. Temperature-morphology correlation for Dark Dune Spots and slope streaks in Richardson crater. Five 100 × 100 m insets from HiRISE images are visible up (from left to right image No. 3175, 3386, 3597, 3742, 3953, which were acquired at Ls = 210.6, 220.7, 230.9, 238.1, 248.5 respectively) and TES based annual temperature values are visible below, where daytime and nighttime temperatures form two curves on the right.

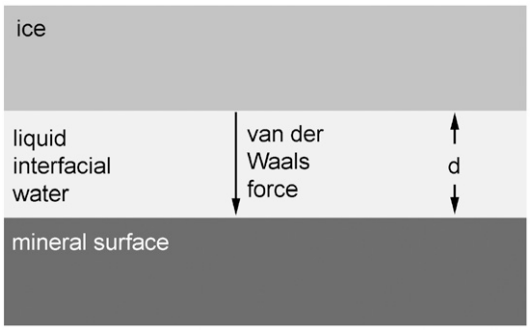

Fig. 9. The "Sandwich model" of liquid interfacial water (layer thickness d) between ice and surface of a mineral grain.

Because of the small number of available HiRISE images of the slope movement phenomena and the lack of continuous data sets, the exact determination of the appearance/disappearance of slope structures is not yet possible. But several important conclusions can already be drawn from the available images. Based on the comparison of images and temperature data from different latitudes, the flow-like (or rheologic) process seems to start when the temperature is above the carbon dioxide frost point, around about 180–200 K. The movements usually take place on a meter scale distance per day. The phenomenon of an undercooled liquid interfacial water layer may help to understand these movements on slopes, as described below.

8. Liquid interfacial water on Mars

Around hydrophilic mineral grains embedded in snow/ice, a layer of liquid interfacial water must form between the mineral surface and the snow/ice (Möhlmann, 2008). The reason is the freezing point depression due to the attractive pressure between the surfaces of water-snow/ice and the mineral. This can also for surfaces of ice (without a mineral counterpart) be described in terms of "premelting" of ice (Dash et al., 2006) by attractive van der Waals force acting upon the uppermost surface layers of snow/ice (cf. Fig. 9).

This attractive van der Waals force F_{vdW}, acting per area F upon the surface of ice of volume $V = Fd$ on a mineral surface F is given in case of parallel interfaces by

$$F_{\mathrm{vdW}} = \frac{A_{\mathrm{llm}}}{6\pi d^3} F. \quad (1)$$

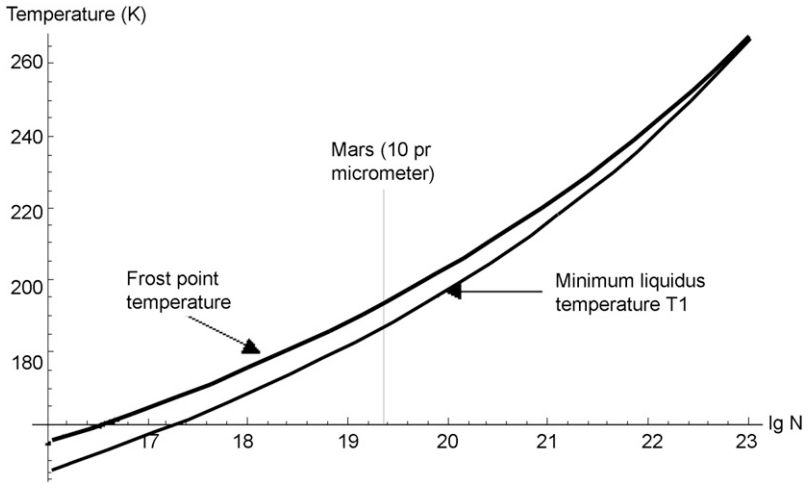

Fig. 10. Frost point temperature (thick line) and minimum liquidus temperature (thin curve below) in dependence on the (log of the) number density N of water vapor molecules (water molecules per cubic meter). The small area between the two curves is the "band of undercooled liquid interfacial water" (Möhlmann, 2008, in T–N-phase space).

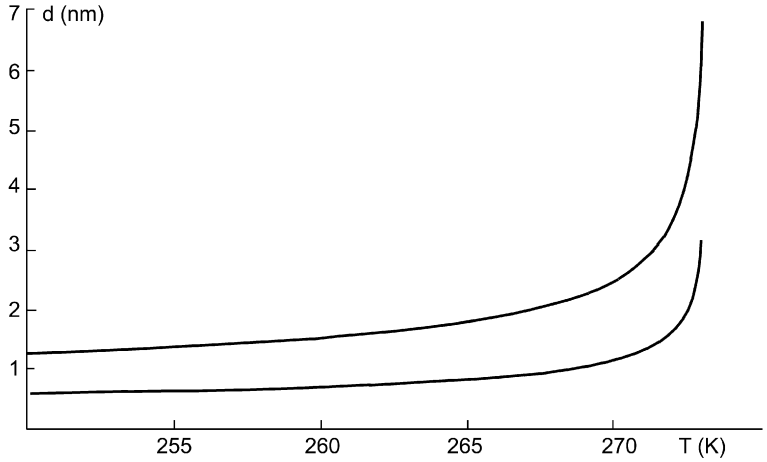

Fig. 11. Dependence of the thickness d [m] of the liquid interfacial water layer on the limiting temperature T_l [K] of undercooled water to remain liquid for two Hamaker constant values: $A = 10^{-18}$ J (upper curve) and $A = 10^{-19}$ J (lower curve).

A_{llm} is the Hamaker constant (Hamaker, 1937) for the interaction of substances "l" (ice) and "m" (mineral) in presence of interfacial water "l" in between. This force acts also between the molecules of water ice at and very near to the surface of ice, which therefore is prone to "premelting". This configuration is described schematically in Fig. 10. The related depressed freezing temperature can in general be shown to be related to different acting pressures, as interfacial melting (premelting) via F_{vdW}, via curvature melting in course of surface tension, and pressure melting via $(p_L - p_m)((\rho_S/\rho_L) - 1)$ by

$$\rho_S q \frac{T_m - T}{T_m} = \frac{A}{6\pi d^3} + \kappa\sigma + (p_L - p_m)\left(\frac{\rho_S}{\rho_L} - 1\right) \tag{2}$$

(cf. Dash et al., 2006; Wettlaufer and Worster, 2006). T_m is the standard melting temperature, $\Delta T = T_m - T$ is called the freezing point depression, q is the latent heat, ρ and p represent mass density and pressure, respectively, and the indices L and S indicate the solid (i.e. ice) and the liquid state.

The limiting minimum temperature of the liquid phase of the water layer below the bulk melting temperature T_m is in case of acting van der Waals forces only, given by

$$T = T_m\left(1 - \frac{A}{6\pi q \rho_S d^3}\right). \tag{3}$$

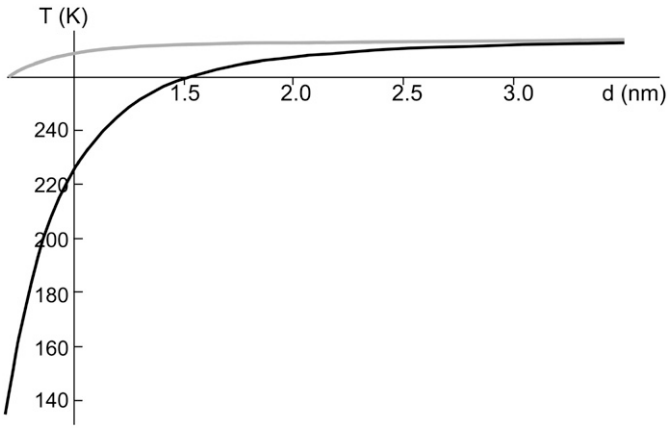

Fig. 12. Minimum liquid layer temperature for $A = 10$–19 J (upper gray curve) and $A = 10$–18 J (lower black curve) in dependence on the layer thickness d. Obviously, liquid interfacial water of about two monolayers in thickness may for appropriate surfaces exist down to about 150 K.

Fig. 11 shows the limiting minimum temperature for interfacial water to remain liquid in dependence on layer thickness and for the range of typical Hamaker constants in nature. As shown in Fig. 12, interfacial water may exist down to about 150 K, as it

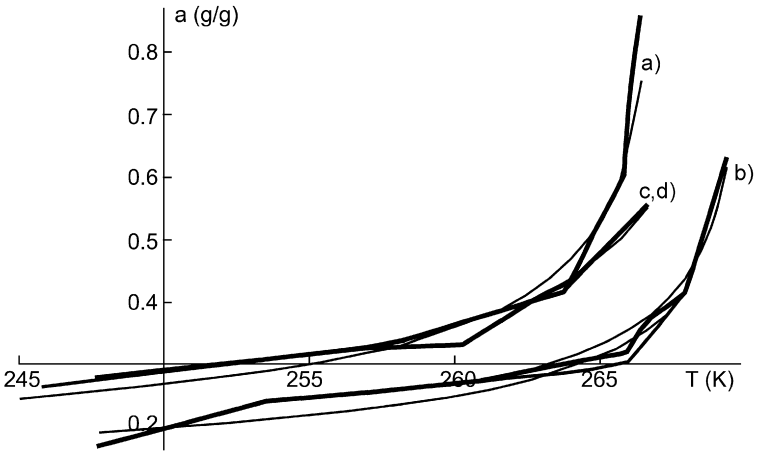

Fig. 13. Li-, Na-, Ca-, and K-montmorillonites (exp.: thick lines, theor.: thin lines), according to experimental data of Anderson (1968) and by using Eq. (5). (a) Li-montmorillonite reaches up to about 0.8 g/g (uppermost curve), (b) Na-montmorillonite reaches up to about 0.65 g/g (lower right curve), (c) Ca-montmorillonite reaches up to about 0.55 g/g, and (d) K-montmorillonite (very similar to Ca-montmorillonite, b) reaches up to about 0.4 g/g (nearly overlapping curves in the middle).

has experimentally been verified by Pearson and Derbyshire (1974). Furthermore, the existence of "unfrozen" water in subzero temperature soils has also been demonstrated and studied by Anderson (1968) and Anderson et al. (1973). Note that the thickness of the layer of undercooled liquid interfacial water is often measured in film-like "monolayers" (of 0.35 nm), which are to be understood as an orienting average value, not as a stringent geometrical model

$$d = \left(\frac{AT_m/6\pi}{\rho_S q \Delta T} \right)^{1/3}. \quad (4)$$

This limiting temperature can get lowered in brines by adding salts, which also tend to increase the thickness d of the layer. Figs. 11 and 12 indicate that liquid interfacial water must exist on Mars in a temperature band below the melting temperature. These temperatures can be reached at polar latitudes at daytime conditions and in the vicinity of the snow/ice interface above an insolation-heated ground, and it can remain "stable" for hours until the ice has left by daytime sublimation or until cooling starts at late afternoon hours (cf. Fig. 12).

Comparatively high sub-surface temperatures, which may approach the melting point (with the consequence of possible temporary melting) can be expected in course of effective cooling at the surface of insolated ice/snow (due to sublimation and RI re-radiation) but with heat accumulation in an insolation-absorbing sub-surface, if the thermal conductivity is sufficient small. At least, this will strengthen the possible appearance and amount of interfacial water.

Undercooled liquid interfacial water will be able to flow downhill on slopes, being that way a driver of rheologic processes, and parts of it also may seep downward into the subsurface. This infiltrated water will refreeze in the cooler lower subsurface layers. Resulting erosion can modify these layers, since ice is of an about 9% larger volume than the liquid interfacial water. The final result will finally be a stress built-up in the upper subsurface. This may lead to cracks, failures and erosive processes (cf. Fisher, 2005).

8.1. Liquid interfacial water in soil

The content of liquid interfacial water in porous soil of specific surface S_M, dry mass m_{dry} and mass $M_{\mathrm{H_2O}}$ of liquid interfacial water can simply be estimated via

$$a_m(T,d) = \frac{M_{\mathrm{H_2O}}(T,d)}{m_{\mathrm{dry}}} = \rho_{\mathrm{H_2O}} S_M d = S_M \rho_{\mathrm{H_2O}} \left(\frac{AT_m}{6\pi q \rho_S \Delta T} \right)^{1/3}. \quad (5)$$

Fig. 13 shows measured and modeled (by Eq. (5)) soil water contents for four different montmorillonites. Obviously, the content of "microscopic", better "nanometric", liquid interfacial water in frozen soil is a macroscopically relevant phenomenon. It may well reach several 10%. This phenomenon is well known as "unfrozen" water in terrestrial permafrost. Analogously to terrestrial permafrost, undercooled liquid interfacial water can on Mars preferably in springtime and after removal of the CO_2-ice cover evolve at sites of the water-ice covered parts of the polar caps in course of their warming.

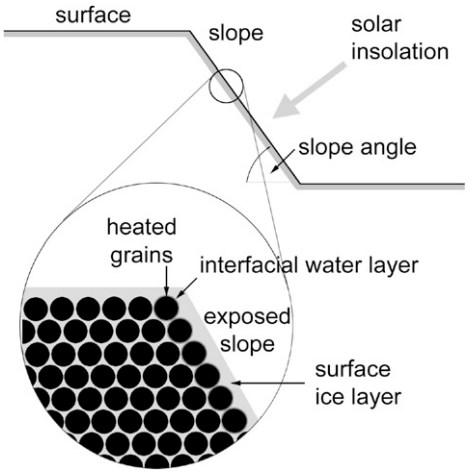

Fig. 14. Geometric slope insulation situation.

8.2. Rheologic phenomena (downslope flows)

The insolated but yet frozen and dark ground on slopes may become the cause of a gravitationally driven flow-like down-slope transport of the interfacial water, preferably between the translucent covering water ice layer and the warmer ground, which is heated by insolation (cf. Fig. 14) towards the melting point temperature. The resulting layer of interfacial water will be able to remain at or near to the melting temperature over longer timespans of hours or so, and thus it must form several monolayers of undercooled liquid interfacial water (cf. Fig. 11). Thus, there can on inclined surfaces, as slopes, form rheologic features as down-flow phenomena. Fig. 14 illustrates that situation. The thickness of that layer is the greatest at temperatures in the vicinity of the melting temperature (cf. Fig. 11). Depending on grain sizes, that can in the 10 nm range (and less) become sufficient also for capillary effects to get involved in this wetting and transport process.

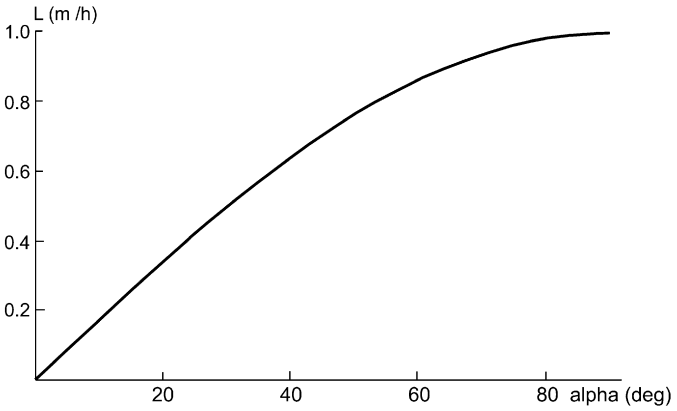

Fig. 15. Maximum diurnal downslope flow distance L [m] in dependence on slope inclination ($R = 10$–5 m, $\rho_P = 3000$ kg m^{-3}, $\rho_W = 1000$ kg m^{-3}).

The flow of liquid interfacial water will be counteracted by friction within the liquid layer. The resulting stationary velocity v of a particle of radius R within the liquid layer is given then by

$$v = \frac{2R^2(\rho_P - \rho_W)g\sin\alpha}{9\eta}. \quad (6)$$

The viscosity η is given by $\eta = 1.38 \times 10^{-3}$ Pa s (Rempel et al., 2001), g is the gravitational acceleration on the surface, α is the inclination of the slope, and ρ_P and ρ_W are the mass densities of the particle and of the water, respectively. Obviously, diurnal downslope flow distances up to about 1 m can be estimated to be reachable in case of the above described slope model (Fig. 15).

Figs. 5–8 give examples of possibly related flow-like features on a martian slope, as observed by HiRISE and studied in the view of the propagation properties by A. Kereszturi et al. at Collegium Budapest (Kereszturi et al., 2008). The diurnal progress is about 1 m, but these flow-like movements can, of course, be effective over only a few hours a day. So, the real propagation velocity in the few daily "active hours" is correspondingly larger. Probably, the presence liquid interfacial water can also have an influence on its optical properties by solving coloring chemical substances from the solid subsurface materials, what can support the heating process further.

8.3. Erosion and failure

In water-filled pores, refreezing of liquid undercooled interfacial water ice will cause erosion. The phase change from liquid water to ice results in volume increase (ΔV) of about $\Delta V/V = 9\%$ and will cause a pressure or elastic stress in the ice/mineral matrix. This stress can cause failure and cracks with erosive results. Therefore, erosion advances in course of refreezing of interfacial water, when the seasonal temperatures approach the local freezing point temperature. In case of the presence of a water ice cover of the surface, seepage and infiltration of interfacial water and its refreezing in the subsurface will happen when the frost point temperature will be reached daytime (in spring) and will decrease below during nighttime.

The erosive stress τ due to refreezing water can be estimated via

$$\tau = \frac{E}{1-2\nu}\frac{\Delta V}{V}. \quad (7)$$

E is Young's modulus, and ν is Poisson's constant. Typical values for snow and water ice are $E \approx (1$–$10) \times 10^9$ Pa, and $\nu \approx 0.2$–0.5 given by Mellon (1975). With $\Delta V/V = 0.09$, this indicates that the related stress can cause erosive destruction around 1 GPa. For materials to fail by brittle structure, there is usually a linear correlation between uniaxial compressive strength σ and Young's modulus with $\sigma/E \approx (2$–$3) \times 10^{-3}$ (Mellon, 1975). Compressive stresses are for snow between (1–10) MPa (Mellon, 1975). Therefore, refreezing driven stresses can become the cause of erosive destruction in ice/snow mixtures.

9. Conclusions

Based on observations, narrow, confined, dark slope streaks emanate from Dark Dune Spots during local spring at the observed three craters. These streaks always start from features called Dark Dune Spots, they stretch and move downward, and follow the topography of the depressions between the small scale ripples, producing a branching pattern. Gravity-driven processes can let streaks grow in time, with a speed up to 1.4 m/sol, as derived from observations. This agrees in the order of magnitude with model estimates. These movements were observed when the temperature was above the carbon dioxide frost point, and up to ~250 K, suggesting that this process is not related to carbon dioxide frost and therefore is possibly connected to liquid interfacial water, if water ice is inside the spots. After the darkening of a certain surface area, brightening may follow as the dark flow front has passed by, probably by refreezing of frost, or the phase change of surface material. Unfortunately today only CRISM data has enough spatial resolution to analyze the possible presence of water ice inside spots, but the publicly available data does not meet the required locations and seasonal periods together.

Taking the assumption that water ice is present inside the spots, interfacial water driven process may produce the observed phenomena. Based on thermodynamics, it can be stated, that interfacial liquid water must, at least temporarily, be present on the martian surface, particularly in the shrinking and warming seasonal water ice covered terrain. Rheologic, flow-like phenomenon at inclined surfaces, which are caused by liquid interfacial water between a covering ice sheet and the warmed-up mineral surface are therefore to be expected to happen on present Mars. As a result, interfacial water may produce change in the appearance of the dune' surface by 1. seeping and causing sublimation of surface frost cover, 2. by produce sliding of lubricated grains above each other and 3. by refreezing produced stress and movement in the grain structure. Our computations and model show that such processes are reasonable under the present surface conditions and satisfactorily interpret the observed movement of springtime streaks. The presence of interfacial water at the observed features even may have astrobiological consequences (Horvath et al., 2001; Ganti et al., 2003; Pocs et al., 2004; Szathmary et al., 2007) too.

Acknowledgments

This work was supported by the ESA ECS-project No. 98076 and the Pro Renovanda Cultura Hungariae Foundation, Student Science Fellowship Award.

References

Aharonson, O., Schorghofer, N., Gerstell, F.M., 2003. Slope streak formation and dust deposition rates on Mars. J. Geophys. Res. 108 (E12), doi:10.1029/2003JE002123. 5138.

Anderson, D.M., 1968. Undercooling, Freezing point depression, and ice nucleation of soil water. Isr. J. Chem. 6, 349–355.

Anderson, D.M., Tice, A.T., McKim, H.L., 1973. The unfrozen water and apparent specific heat capacity of frozen soils. In: North American Contribution, Permafrost, Second Int. Conference, Yakutsk. National Academy of Sciences, Washington, DC, pp. 289–296.

Beyer, R.A., Chuang, F.C., Thomson, B.J., Milazzo, M.P., Wray, M.P., 2008. Martian slope streak brightening mechanisms. Lunar Planet. Sci. 39. Abstract 2538.

Bibring, J.P., Langevin, Y., Poulet, F., Gendrin, A., Gondet, B., Berthe, M., Soufflot, A., Drossart, P., Combes, M., Bellucci, G., Moroz, V., Mangold, N., Schmitt, B., and

the OMEGA Team, 2004. Perennial water ice identified in the south polar cap of Mars. Nature 428, 627–630.
Bibring, J.P., Langevin, Y., Gendrin, A., Gondet, B., Poulet, F., Berthe, M., Soufflot, A., Arvidson, R., Mangold, N., Mustard, J., Drossart, P., and the OMEGA Team, 2005. Surface diversity as revealed by the OMEGA/Mars Express observations. Science 307, 1576–1581.
Brass, G.W., 1980. Stability of brines on Mars. Icarus 42, 20–28.
Christensen, P., Anderson, D., Chase, S.C., Clark, R.N., Kieffer, H.H., Malin, M.C., Pearl, J.C., Carpenter, J.B., Nuno, B.F., 1992. Thermal emission spectrometer experiment: Mars observer mission. J. Geophys. Res. 97, 7719–7734.
Christensen, P.R., Kieffer, H.H., Titus, T.N., 2005. Infrared and visible observations of south polar spots and fans. Eos (Fall Meeting) 86. Abstract P23C-04.
Chuang, F.C., Beyer, R.A., McEwen, A.S., Thomson, B.J., 2007. HiRISE observations of slope streaks on Mars. Geophys. Res. Lett. 34 (20), doi:10.1029/2007GL031111. L20204.
Clow, G.D., 1987. Generation of liquid water on Mars through the melting of a dusty snowpack. Icarus 72, 95–127.
Dash, J.G., Rempel, A.W., Wettlaufer, J.S., 2006. The physics of premelted ice at its geophysical consequences. Annu. Rev. Fluid Mech. 38, 427–452.
Fisher, D.A., 2005. A process to make massive ice in the martian regolith using long-term diffusion and thermal cracking. Icarus 179, 387–397.
Ganti, T., Horvath, A., Berczi, Sz., Gesztesi, A., Szathmary, E., 2003. Dark dune spots: Possible biomarkers on Mars? Origins Life Evol. Biosphere 33, 515–557.
Ganti, T., Berczi, Sz., Horvath, A., Kereszturi, A., Pocs, T., Sik, A., Szathmary, E., 2006. Hypothetical time sequence of the morphological changes in global and local levels of the dark dune spots in polar regions of Mars. Lunar Planet. Sci. 37. Abstract 1918.
Haberle, R.M., McKay, C.P., Schaeffer, J., Cabro, N.A., Grin, E.A., Zent, A.P., Quinn, R., 2001. On the possibility of liquid water on present-day Mars. J. Geophys. Res. 106 (E10), 23317–23326.
Hamaker, H.C., 1937. The London–van der Waals attraction between spherical particles. Physica IV 10, 1058–1072.
Head, J.W., Marchant, D.R., Dickson, J.L., Levy, J.S., Morgan, G.A., 2007a. Slope streaks in the Antarctic Dry Valleys: Characteristics, candidate formation mechanisms, and implications for slope streak formation in the martian environment. In: 7th International Conf. on Mars. Abstract 3114.
Head, J.W., Marchant, D.R., Dickson, J.L., Levy, J.S., Morgan, G.A., Kreslavsky, M., 2007b. Mars gully analogs in the Antarctic Dry Valleys: Geological settings and processes. In: 7th International Conf. on Mars. Abstract 3118.
Hecht, M.H., 2002. Metastability of liquid water on Mars. Icarus 156, 373–386.
Horvath, A., Ganti, T., Gesztesi, A., Berczi, Sz., Szathmary, E., 2001. Probable evidences of recent biological activity on Mars: Appearance and growing of dark dune spots in the south polar region. Lunar Planet. Sci. 32. Abstract 1543.
Horvath, A., Kereszturi, A., Berczi, Sz., Sik, A., Pocs, T., Gesztesi, A., Ganti, T., Szathmary, E., 2005. Annual change of martian DDS-seepages. Lunar Planet. Sci. 35. Abstract 1128.
Horvath, A., Kereszturi, A., Berczi, Sz., Sik, A., Pocs, T., Ganti, T., Szathmary, E., 2009. Analysis of dark albedo features on a Southern Polar dune field of Mars. Astrobiology 9 (1).
Kereszturi, A. Sik, Horvath, A., Reiss, D., Jaumann, R., Neukum, G., 2007. Season-dependent behavior of Dark Dune Spots on Mars. Lunar Planet. Sci. 38. Abstract 1864.
Kereszturi, A., Möhlmann, D., Berczi, Sz., Horvath, A., Ganti, T., Kuti, A., Pocs, T., Sik, A., Szathmary, E., 2008. Analysis of possible interfacial water driven seepages on Mars. Lunar Planet. Sci. 39. Abstract 1555.
Kieffer, H.H., 2003. Behavior of solid CO_2 on Mars: A real zoo. In: 6th International Conf. on Mars. Abstract 3158.
Kieffer, H.H., Titus, T.N., 2001. TES mapping of Mars' north seasonal cap. Icarus 154, 162–180.
Kieffer, H.H., Christensen, P.R., Titus, T.N., 2006. CO_2 jets formed by sublimation beneath translucent slab ice in Mars' seasonal south polar ice cap. Nature 442, 793–796.
Knauth, L.P., Burt, D.M., 2002. Eutectic brines on Mars: Origin and possible relation to young seepage features. Icarus 158, 267–271.
Kossacki, K.J., Markiewicz, W.J., 2008. Martian hill-gullies, surface and sub-surface moisture. In: Mars Water Cycle Workshop, Paris. Oral presentation.
Langevin, Y., Bibring, J.P., Douté, S., Vincendon, M., Poulet, F., Gondet, B., Schmitt, B., Forget, F., Montmessin, F., and the OMEGA Team, 2006. CO_2 ice and H_2O ice in the seasonal caps of Mars during the spring retreat, phase. In: 4th Mars Polar Sci. Conf. Abstract 8091.
Malin, M.C., Edgett, K.S., 2000. Frosting and defrosting of martian polar dunes. Lunar Planet. Sci. 31. Abstract 1056.
Mellon, M., 1975. A review of basic snow mechanics. In: Snow Mechanics Symposium, vol. 251. IAHS Publ. 114.
Mellon, M.T., Phillips, R.J., 2001. Recent gullies on Mars and the source of liquid water. J. Geophys. Res. 106, 1–15.
Motazedian, T., 2003. Currently flowing water on Mars. Lunar Planet. Sci. 34. Abstract 1840.
Möhlmann, D., 2004. Water in the upper martian surface at mid- and low-latitudes: Presence, state, and consequences. Icarus 168, 318–323.
Möhlmann, D., 2008. The influence of van der Waals forces on the state of water in the shallow subsurface of Mars. Icarus 195, 131–139.
NASA Press Release, 2008. No. 08-246, 2008.09.29.
Pearson, T.T., Derbyshire, W., 1974. NMR studies of water adsorbed on a number of silica surfaces. J. Colloid Interface Sci. 46 (2), 232–248.
Piqueux, S., Byrbe, S., Richardson, M.I., 2003. Sublimation of Mars' southern seasonal CO_2 ice cap and the formation of spiders. J. Geophys. Res. 108. 5084.
Pocs, T., Horvath, A., Ganti, T., Berczi, Sz., Szathmary, E., 2004. Possible crypto-biotic-crust on Mars? In: Exo/Astrobiology, Proc. Third Eur. Workshop. ESA SP-545, pp. 265–266.
Rempel, A.W., Wettlaufer, J.S., Worster, M.G., 2001. Interfacial premelting and the thermomolecular force: Thermodynamic buoyancy. Phys. Rev. Lett. 87 (8), 088501–088504.
Schmitt, B., Douté, S., Langevin, Y., Forget, F., Bibring, J.P., Gondet, B., and the OMEGA Team, 2005. Northern seasonal condensates on Mars by Omega/Mars Express. Lunar Planet. Sci. 6. Abstract 2326.
Schmitt, B., Schmidt, F., Douté, S., Langevin, Y., Forget, F., Bibring, J.P., Gondet, B., and the OMEGA Team, 2006. Recession of the northern seasonal condensates on Mars by OMEGA/Mars Express. In: 4th Mars Polar Sci. Conf. Abstract 8050.
Schorghofer, N., Aharonson, O., Gerstell, M.F., Tatsumi, L., 2007. Three decades of slope streak activity on Mars. Icarus 191, 132–140.
Smith, D., Neumann, G., Ford, P., Arvidson, R.E., Guinness, E.A., Slavney, S., 1999. Mars Global Surveyor Laser Altimeter Precision Experiment Data Record. NASA Planetary Data System, MGS-M-MOLA-3-PEDR-L1A-V1.0.
Szathmary, E., Horvath, A., Sik, A., Berczi, Sz., Ganti, T., Pocs, T., Kereszturi, A., 2005. Signs of water runoff and its relation to possible living organisms on Mars. In: 5th EANA Workshop on Astrobiology, Budapest.
Szathmary, E., Ganti, T., Pocs, T., Horvath, A., Kereszturi, A., Berzci, Sz., Sik, A., 2007. Life in the dark dune spots of Mars: A testable hypothesis. In: Pudritz, R., Higgs, P., Stone, J. (Eds.), Planetary Systems and the Origin of Life. Cambridge University Press, Cambridge, UK.
Titus, T.N., 2005. Thermal infrared and visual observations of a water ice lag in the Mars southern summer. Geophys. Res. Lett. 32 (24), doi:10.1029/2005GL024211. L24204.
Titus, T., 2008. Infrared observations of Mars south polar water ice. In: Mars Water Cycle Workshop, Paris.
Wagstaff, K.L., Titus, N.T., Ivanov, A.B., Castano, R., Bandfield, J.L., 2008. Observation of the north water ice annulus on Mars using THEMIS and TES. Planet. Space Sci. 56, 256–265.
Wettlaufer, J.D., Worster, M.G., 2006. Premelting dynamics. Annu. Rev. 38, 427–452.